Core ideas:

- Six portable soil moisture systems showed accurate performance after site-specific correction
- Soil Moisture data from similar electrode length sensors showed statistically similar soil moisture distribution
- Synergetic use of two different sensor types can greatly improve the correlation coefficient and reduce systematic bias

Field Evaluation of Portable Soil Water Content Sensors in a Sandy Loam

Hyunglok Kim[1], Michael H. Cosh[2], Rajat Bindlish[3], and Venkataraman Lakshmi[1]

[1]Department of Earth Systems and Environment, University of Virginia, Charlottesville, VA 22904, USA

[2]USDA ARS Hydrology and Remote Sensing Lab, Beltsville, MD 20705, USA

[3]NASA Goddard Space Flight Center, Greenbelt, MD 20771, USA

Corresponding author: Hyunglok Kim (hk5kp@virginia.edu; ORCID: 0000-0002-5790-7012)

Michael H. Cosh (Michael.Cosh@ars.usda.gov; ORCID: 0000-0003-4776-1918

Rajat Bindlish (rajat.bindlish@nasa.gov; ORCID: 0000-0002-1913-0353)

Venkataraman Lakshmi (vlakshmi@virginia.edu; ORCID: 0000-0001-7431-9004)

Abbreviations:

EC, electrical conductivity; EM, electromagnetic; SM, soil moisture; R, correlation coefficient; RMSD, root mean square difference; TDR, time domain-reflectometry; FDR, frequency domain-reflectometry; TLO, transmission line oscillation; ubRMSD, unbiased root mean square difference; VWC, volumetric water contents; GVWC, gravimetric-based volumetric water contents

3. Apr. 2020

Abstract

Ground observations are critical in the validation of soil water content (SWC) estimates from both satellites and land surface models. Portable SWC sensors provide useful information to determine the amount of SWC in the topsoil layer for various applications; however, these probes are not accurate without site-specific calibration. In the present study, we examined and compared 6 different types of portable electromagnetic (EM) soil water content sensors, including multiple sensors made by the same manufacturers, for a total of 16 EM-based SM probes equipped with portable data loggers. All SM probes met the target accuracy after on-site calibration - the Root Mean Square Difference (RMSD) was less than 0.025 m^3m^{-3}. Using the two-sample *t*-tests, we observed that SWC data obtained from similar electrode lengths and from different manufacturers showed similar distributions over time with the same mean. Furthermore, using the maximize R method to combine SM data from two different types of sensors increased the accuracy of the results. When datasets from two different types of sensors were combined, the Pearson's correlation coefficient (R-value) and RMSD values were improved the average R-value improved from 0.930 to 0.945, and the RMSD decreased from 0.036 m^3m^{-3} to 0.018 m^3m^{-3}. These results indicate that, along with site-specific calibration, synergetic use of multiple manufacturers' EM-based SWC probes can improve the R-value and reduce systematic bias.

1 Introduction

Portable devices are an effective tool for measuring surface soil water content (SWC). They can also serve as an alternative to gravimetric sampling as the electromagnetic (EM) properties of soil vary according to the water content in the soil (Topp, 2003) and these devices provide reasonably accurate measurements and avoid the cumbersome collection and drying issues related to gravimetric sampling. Over the last several decades, many portable electromagnetic-based sensors have been developed to estimate volumetric water content in porous media in an efficient manner (Birchak et al., 1974; Lee and Fredlund, 1984; Topp, 2003; Seyfried and Murdock, 2004; Vaz et al., 2013; Rowlandson et al., 2013; Singh et al., 2018). EM-based SWC probes have shown several advantages over other techniques; for instance, SWC probes are less invasive and cumbersome than gravimetric techniques, they are suitable for long-term and continuous monitoring of SWC at specific depths, they can be used in most surface conditions regardless of soil types and vegetation, and they can collect SWC data repeatedly (Blonquist et al., 2005; Evett et al., 2006; Abbas et al., 2011; Vaz et al., 2013).

However, SWC probes must be calibrated for farmland management and for validation of remotely-sensed SWC retrievals (Robinson et al., 2003; Cosh et al., 2005) and for different soil types as soil properties affect EM-based SWC measurement (Malicki et al., 1996; Ponizovsky et al., 1999; Leib et al., 2003). Thus, soil-specific correction is recommended for SWC probes before application even though factory-determined calibration options are generally employed due to their simplicity. Many previous studies have described EM sensor applications in different soils and have compared SWC probes in laboratory settings (Walker et al., 2004; Blonquist et al., 2005; Evett et al., 2006; Chow et al., 2009; Vaz et al., 2013). However, few studies has intercompared the performance of

69 portable EM-based SWC probes made by different manufacturers, and even fewer studies
70 have combined two different EM-based SWC data sets with the aim of improving the
71 accuracy of SWC measurement at field scales.

72 In the present study, we focus on the evaluation, correction, and combination of six types
73 of portable SWC probes in a portable configuration with handhel data loggers. We chose the
74 following probes because they have been widely used both by farmers and by scientists in
75 various research fields of study: the ThetaProbe Soil Moisture Sensor (hereafter ML3), the
76 HydraProbe Soil Moisture Sensor (hereafter HydraProbe), the Spectrum TDR100 Soil
77 Moisture Meter (hereafter FS100), the SM150 Soil Moisture Sensor (hereafter SM150), the
78 HydroSense II Portable System (hereafter HS2), and the TRIME-PICO64 Probe (hereafter
79 PICO64). An analysis of the performance of these probes is necessary for a variety of
80 applications as some projects cannot support the deployment of in-situ loggers. Spatial
81 assessments of SWC are more efficiently performed with portable sensors as is the case with
82 the major soil moisture field experiments Soil Moisture Experiments (SMEX) (Bosch et al.,
83 2006), SMAPVEX (Jackson et al., 2012), National Airborne Field Experiment (NAFE)
84 (Mladenova et al., 2011), and Canadian Experiment for Soil Moisture (CANEX) (Magagi et
85 al., 2013). Individual assessments of the sensors used in these campaigns have been
86 performed, but this is the first cumulative assessment of all common sensors examined for a
87 single soil type as a common basis of comparison. To investigate the accuracy of these six
88 SWC probes, the data were collected in sandy loam soil at a research site in Maryland, USA,
89 in the summer of 2019. The present research seeks to answer the following questions: 1)
90 What are the measurement uncertainties of various commercially-available portable SWC
91 sensors? 2) Do different types of SWC probes, or several probes of the same type, show
92 statistically different performance in comparison with reference data? 3) Can we improve

the performance of SWC sensors by combining data from different type of sensors? Answering these questions will provide us with new insights into the characteristics, limitations, and uncertainties of different SM probes with portable devices.

2 Study Site

The Optimizing Production Inputs for Economic and Environmental Enhancement (OPE3) site is located in Prince George's County, Maryland, USA (Geographical coordinates: Latitude 39.03˚, Longitude -76.84˚). Since 1998, over 90 scientists from several U.S. federal agencies, universities, and private industry have conducted research at this location (De Lannoy et al., 2006; Srivastava et al., 2015). This site is listed in the Soil Climate Analysis Network (SCAN) as Powder Mill (https://www.wcc.nrcs.usda.gov/scan/). The soil texture at the OPE3 site is sandy loam with 56% of the site classified as the Russett-Christian complex. The field texture of the soil was determined based on particle-size distribution analysis. Further information regarding the soil texture of the OPE3 site is shown in **Figure 1a** and **Table 1**. The thirty locations from which soil samples were taken are marked with red boxes (**Figure 1(a)**). More detailed descriptions of each sampling location are shown in **Figure 1(b),** and further information on how the process used to obtain the soil samples is provided in the methodology section.

Table 1. Summarization of the soil texture at the OPE3 site.

Depth (cm)	Texture	Clay	Silt	Sand
0-14		5.7	23.9	70.4
14-29	Sandy Loam	6.3	25.9	67.8
29-46		6.2	30.8	63.0

https://ncsslabdatamart.sc.egov.usda.gov/

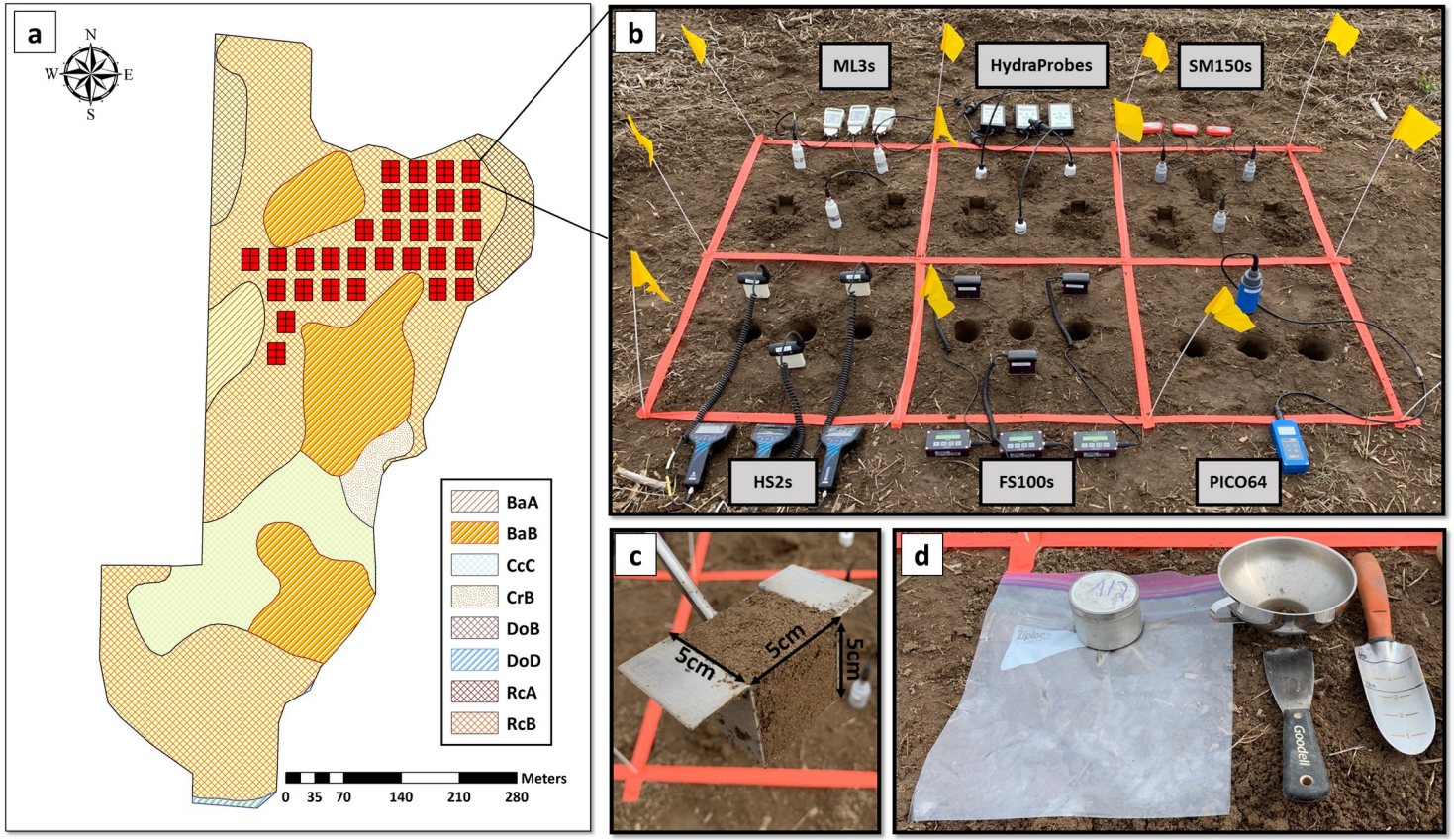

BaA Beltsville silt loam, 0 to 2 percent slopes
BaB Beltsville silt loam, 2 to 5 percent slopes
CcC Christiana-Downer complex, 5 to 10 percent slopes
CrB Croom gravelly sandy loam, 2 to 5 percent slopes
DoB Downer-Hammonton complex, 2 to 5 percent slopes

Figure 1. (a) The soil map of the OPE3 site: the thirty red boxes indicate sampling locations. The actual sampling boundary was about 2.1-m by 1.4-m, and a gap of at least 20-m from the center of each sampling point was ensured between different soil types. (b) One of the sampling locations at the OPE3 site. (c) The scoop tool (5 cm×5 cm×5 cm) and funnel (inset picture) used to sample 0-5 cm soils. (d) Can, bag, funnel, spatula, and depth-marked hand shovel. Note: the shovel was used to

3 Datasets

The relative permittivity of soil is primarily dependent on water content and secondarily on temperature, bulk electrical conductivity, clay content and type, and electromagnetic frequency (Robinson et al., 2003; Seyfried et al., 2005; Logsdon et al., 2010). The relative permittivity is defined as the ratio of the dielectric of the material to that of the voids. The real part of the soil dielectric describes its ability to store energy in an applied electric field while the imaginary part relates to energy loss (Topp et al., 1980; Bosch, 2004). Estimates of the real component of the dielectric are often described as the apparent dielectric (K_a) as estimates neglect the energy loss components (Bosch, 2004). The effective frequency range for measuring SWC is based on the dielectric number of the saturated soil known to lie approximately between 50 MHz and 10,000 MHz (Vaz et al., 2013). If the frequency is below 100 MHz, the relative permittivity of moist soil depends greatly on soil type (Smith-Rose, 1935); and if the frequency is above 10,000 MHz, the relative permittivity of moist soil falls off due to water relaxation (Hoekstra and Delaney, 1974; Roth et al., 1990). Many impedance and capacitance sensors operate at lower frequencies between 20-300 MHz (Bosch, 2004); and time domain reflectometry (TDR), time domain-transmissometry (TDT), and transmission line oscillation (TLO) operate within the frequency range between 100 MHz and 10 GHz (Topp et al., 1980; Cassel et al., 1994; Heimovaara et al., 1996; Vaz et al., 2013).

In this study, we investigated six different portable EM-based SWC probes with portable data loggers (**Figure 2**), using multiple sensors of the same type and testing 16 SWC probes in all. It is worth noting that while these this study tested probes equipped with portable data loggers in this study,, the performance results of the probes will be analogous to an in situ installation. The total number of sensors included three ML3 ThetaProbe Soil Moisture sensors (Delta-T Devices Ltd, Cambridge, UK) (section 3.1); three HydraProbe soil moisture

sensors (Stevens Water Monitoring Systems, Inc. Oregon, USA) (section 3.2); three FS100 (Spectrum) sensors (Spectrum Technologies, Inc. IL, USA) (section 3.3); three SM150 Soil Moisture sensors (Delta-T Devices Ltd, Cambridge, UK) (section 3.4); three HydroSense II sensors (Campbell Scientific, Utah, USA) (section 3.5); and one TRIME-PICO64 sensor (IMKO, Germany) (section 3.6). All 16 sensors were tested at the OPE3 site in Maryland, USA. Model numbers, manufacturers, and descriptive information for all sensors are presented in **Table 2**.

All sensor electrodes were inserted perpendicularly into the soil surface until the electrodes were fully covered by soil. Then, factory-determined volumetric water content (VWC) values were taken by reading values shown in the datalogger display.

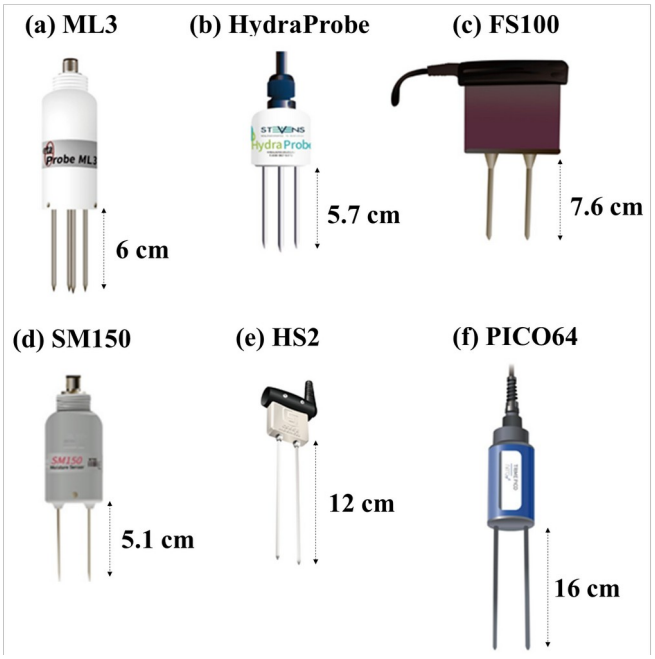

Figure 2. Six portable EM sensors and electrode lengths. The probes used are as follows: (a) three ML3s, (b) three HydraProbes, (c) three FS100s, (d) three SM150s, (e) three HS2s, and (f) one PICO64.

151 **Table 2**. Summarization of specs and related websites for each sensor

Sensor	Abbreviation	Manufacturer	Type	*f*(MHz)	Manufacturer's estimated accuracy	Length of sensing rods
ThetaProbe Soil Moisture Sensor	ML3	Delta-T	I	100	±1% (VWC) over 0 to 50% and 0-40ºC	6 cm
HydraProbe Soil Moisture Sensor	HydraProbe	Stevens	I	50	3% (WFV) and ±0.3% (WFV precision)	5.7 cm
TDR100 Soil Moisture Meter	FS100	Spectrum Tech.	TLO	N/A	±1% (VWC) with electrical conductivity < 2 dS m-1	7.6 cm
SM150 Soil Moisture Sensor	SM150	Delta-T	C	100	±3% (VWC) over 0 to 70% VWC and 0-60°C	5.1 cm
HydroSense II Portable System	HS2	Campbell	TLO	175	±3% (VWC)	12 cm
TRIME-PICO64 Probe	PICO64	IMKO	TLO	1,000	±2% (VWC) over 0 to 40% VWC and ±3% VWC over 40 to 70% VWC	16 cm

152 TDR, time domain reflectometry; TLO, transmission line oscillation; I, impedance; C, capacitance; N/A, not available. The effective
153 frequency is not provided by manufacturers

3.1 The ThetaProbe Soil Moisture Sensor (ML3)

The ML3 ThetaProbe (Delta-T Devices Ltd, Cambridge, UK) is an impedance type sensor designed to measure the relative permittivity of soil (**Figure 2(a)**). ML3 sensors have been used both as portable sensors and as *in situ* sensors buried in the soil for long term studies. Four electrodes are attached to the sealed plastic body, and these electrodes are inserted directly into the soil to measure voltage (mV). The manufacturer's specification of the sensing volume is >95% influence within a 40 mm diameter cylinder, 60mm long, around the central rod. In this study, the linearization table was set to "Mineral" type of soil. Further details regarding the ML3 sensor are provided in the supplemental materials file.

3.2 The HydraProbe Soil Moisture Sensor (HydraProbe)

The Stevens HydraProbe Soil Moisture Sensor (Stevens Water Monitoring Systems, Inc., Oregon, USA) is an electrical impedance sensor designed to determine the relative permittivity of soil using EM waves at a frequency of 50 MHz (**Figure 2(b)**). It has proven to be robust under various field conditions (Seyfried and Murdock, 2004) and has been used both as a portable sensor and as part of in *in situ* SM networks; for example, SCAN in the U.S.A. and REMEDHUS in Spain have adopted the HydraProbe for long-term SWC monitoring (Sanchez et al., 2012; Lievens et al., 2015). The sensors were buried for periods of several months to years to assess sensor performance (Bosch et al., 2006; Cosh et al., 2016) or for application in various research fields (Cosh et al., 2008; Kelleners and Norto, 2012; Hottenstein et al., 2015; Dumedah et al., 2015). The manufacturer's specification of the sensing volume is within a 30 mm diameter cylinder, 57 mm long, around a central rod. In this study we used the Stevens Hydra Data Reader: three HydraProbes were logged into three

177 Stevens Hydra Data Readers. The Hydra Data Reader provides four user-selectable soil
178 texture settings: Sand, Silt, Clay, and Loam. In this study, the soil type was set to Sand as is
179 common for the OPE3 field. Further details regarding the HydraProbe sensor are provided in
180 the supplemental material file.

181

182 **3.3 The Fieldscout TDR100 Soil Moisture Meter (FS100)**

183 The Fieldscout TDR100 (Spectrum Technologies, Inc. IL, USA) is a water content
184 reflectometer (WCR) based on the TLO principle (**Figure 2(c)**). The name "TDR100" would
185 lead the reader to assume that the unit uses TDR, but in reality it does not use TDR (Time
186 Domain Reflectometry). Despite its name, the TDR100 is a WCR-type device (Kargas and
187 Kerkides, 2008; Benor et al., 2013). The K_a is related to the period of applied voltage, which
188 is measured from the WCR. For more details regarding the WCR, please refer to (Chandler et
189 al., 2004). The FS100 technique is similar to that of the Campbell CS616: it uses a quadratic
190 equation related to a period average to calculate SWC (Singh et al., 2018). Very few studies
191 are publicly available regarding comparative research of the FS100 sensors with other SM
192 probes, performance assessment over various soils, or performance assessment over soils
193 having different physicochemical characteristics. The FS100 is suitable for these purposes as
194 it was originally designed for use with portable devices for periodic monitoring and recording
195 of SWC, rather than for use in continuous monitoring of SM *in situ* networks. The
196 manufacturer's specification of the sensing volume is an elliptical cylinder extending
197 approximately 10 mm around the rods. In this study, we used three FS100 sensors (7.6 cm
198 rods) with the VWC setting of Standard Mode. Further details regarding the FS100 sensor are
199 provided in the supplemental materials file.

3.4 The SM150 Soil Moisture Sensor (SM150)

The SM150 Soil Moisture Sensor (Delta-T Devices Ltd, Cambridge, UK) is a capacitance sensor designed to estimate SWC from a differential analog DC voltage (**Figure 2(d)**). SM150 sensors have been used both as portable sensors and as sensors buried in the ground. These sensors have been buried for periods of several days to years in order to collect SWC data for application in various fields of research (Roets et al., 2013; Veeramanikandasamy et al., 2014); however, no performance assessment has been conducted involving use of the SM150 as a portable sensor. The manufacturer's specification of the sensing volume for best results is an elliptical cylinder extending approximately 25 mm around the rods. In this study, we used three SM150 SWC probes with three HH150 dataloggers manufactured by Delta-T Devices Ltd, Cambridge, UK. The HH150 meter provides five default soil texture settings: Mineral, Peat Mix, Coir, Mineral Wool, and Perlite. In this study, the soil type was set to Mineral. Further details regarding the SM150 sensor are provided in the supplemental materials file.

3.5 The HydroSense II Portable System with CS659 (HS2)

The CS659 Water Content Sensor for HydroSense II (Campbell Scientific, Utah, USA) is a 12 cm electrode version of the CS65x (e.g., CS650/655), and all CS65x are new versions of the original CS615 WCR (**Figure 2(e)**) (Caldwell et al., 2018). It is worth noting that all the new CSI TLO are referred to as “CS65x”. The CS65x has been used in various research fields which require ground-based SM measurements; for instance, it was used in optimizing satellite-based SWC data (Bai et al., 2016), investigating tree establishment conditions

(Morrison et al., 2019), and validating satellite- and model-based SWC data (Caldwell et al., 2018, 2019; Moller et al., 2018). In this study, we used the CS659 (12 cm electrode length) with the HydroSense II portable device. The manufacturer's specification of the sensing volume is a cylinder of approximately 30 mm diameter along the full length of the rods. We used three HS2 probes. Further details regarding the CS65x sensor are provided in the supplemental materials file.

3.6 The TRIME-PICO64 Probe

The time domain reflectometry with intelligent micromodule element (TRIME)-PICO64 (hereafter PICO64) sensor is WCR and determines VWC, temperature, and EC in soils (**Figure 2(f)**). The PICO64 sensor is ideal for mobile use with the portable measuring device HD2. The PICO64 been used as a permanent sensor requiring burial for long periods of time; however, no performance assessment has been made regarding this sensor. In contrast to conventional TDR systems, the TRIME system does not determine transit time from the entire waveform; rather, it determines transit time from the time of reflection at a given (threshold) voltage level (amplitude) (Dettmann and Bechtold, 2018). The manufacturer's specification of the sensing volume is approximately 2 mm in the vicinity of the probe rods. In this study, we logged a PICO64 sensor (IMKO, Germany) into an HD2 data logger because PICO64 requires an external 7-24 V/DC power supply. Further details regarding the PICO64 sensor are provided in the supplemental materials file.

4 Methodology

4.1 Gravimetric Water Content

In the present study, we used gravimetric water content (GWC) as the reference for SWC since the thermo-gravimetric method, which consists of collecting and oven-drying the soil, has been considered to produce the most reliable SWC value (Reynolds, 1970; Bosch, 2004). The collected GWC values were converted to VWC units since the probes used in this study use the EM method to determine VWC. The GWC, which is provided in units of g/g, was converted to volumetric units by estimating the ratio of water volume in the soil (called the bulk density of the soil, ρ_b; g/cm^3) to the ratio of the estimated soil sample volume. The GWC is converted to VWC using Eq. [1a]

$$VWC = GWC \frac{\rho_b}{\rho_w} \quad [1a]$$

Where ρ_w is the density of water. In the present study, in order to convert the gravimetric SWC values to VWC--hereafter GVWC--we used the soil scoop and coring tools to collected soil samples from the 30 different points at the OPE3 site where we tested the 16 sensors;. and we collected The soil samples were also used to determine the ρ_b values for depths of 0-5 cm, 0-10 cm, 0-15 cm, and 0-20 cm (Reynolds, 1970; Bosch, 2004). **Figure 3** illustrates the boxplots of ρ_b values with respect to the different depths sampled at OPE3. From **Figure 3**, it is clear that the most accurate GVWC values can be obtained by using different ρ_b values to convert gravimetric SWC values into VWC for different soil depths. For the GVWC values used as references for the ML3s (electrode length: 6 cm), HydraProbes (electrode length: 5.7 cm), and SM150s (electrode length: 5.1 cm) sensors, we used the median values of the 0-5 cm ρ_b. Similarly, for the FS100s, HS2s, and PICO64, we used the median values of 0-10 cm, 0-10 cm, and 0-15 cm ρ_b, respectively, to convert gravimetric SWC to VWC. This conversion was necessary because the electrode lengths of these sensors are 7.6 cm, 12 cm, and 16 cm, respectively. For the soil depth of 0-5 cm, the scoop tool was used to determine the ρ_b value

directly because this tool was specially designed to sample soil in the topsoil layer (5 cm × 5 cm × 5 cm) (**Figure 1(c)**). However, in order to sample deeper soils (i.e., depths of 7.6 cm, 12 cm, and 16 cm), it was necessary to use the coring tool to determine ρ_b values.

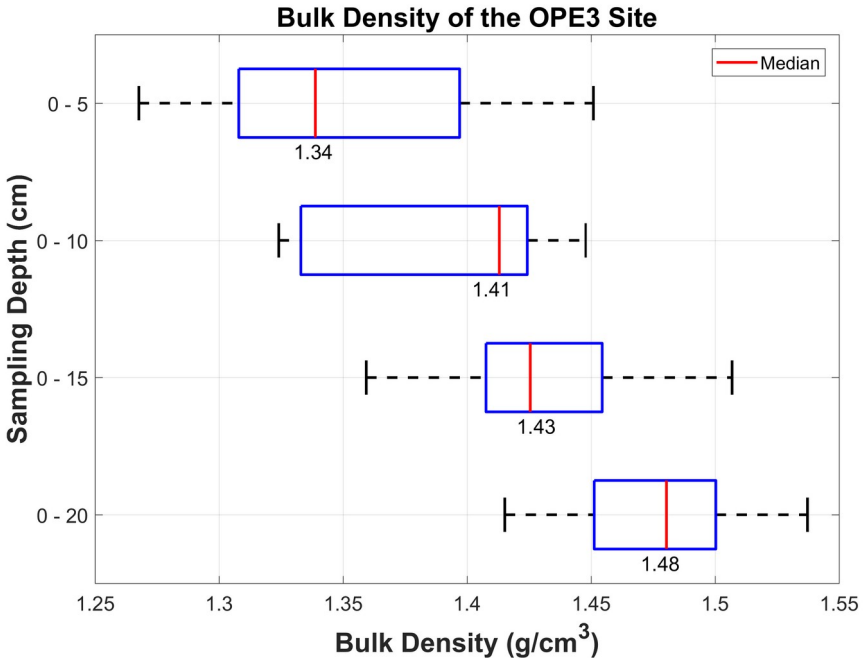

Figure 3. Boxplot showing the bulk density (ρ_b) values for different depths at the OPE3 site. The central red line indicates the median, and the left and right edges of the box represent the 25th and 75th percentiles, respectively. The whiskers extend to the farthest data points not considered as outliers.

4.2 Site-specific Sensor Correction

All 16 sensor readings and all soil samples were taken at the point scale from thirty locations at the OPE3 site (**Figure 2(b)**). Each sensor was tested within a rectangular grid (70 cm × 70 cm), and three soil samples were taken for each sampling. For example, the VWC estimates from the ML3 (electrode length: 6 cm), HydraProbe (electrode length: 5.7 cm), and

SM150 (electrode length: 5.1 cm) sensors were compared with the GVWC values taken from soil samples using a scoop tool with a fixed volume (the scoop tool is shown in **Figure 2(c)**). Similarly, for the FS100, HS2, and PICO64 sensors, we sampled the soil from depths of 0-8 cm, 0-12 cm, and 0-16 cm to obtain the GVWC (using the hand shovel shown in **Figure 2(d)**). To cross-check the sample depth against the length of the electrodes, we measured the depth of the hole after removing the sample. The GVWC sampling location was always less than 10 cm from the location where the probe was inserted (The location of holes and sensors can be seen in **Figure 2(b)**).

To reduce random errors, we averaged the GVWC values obtained from the three soil samples taken at each different sensor type's specific depth. Since we collected three soil samples from 30 locations for the 6 different types of sensors, we obtained a total of 540 soil samples (**Figure 2(b)**). In order to prevent soil drying between the time each sample was taken and the time it was first weighed, we used cans and sealable zipper storage bags (Ziploc) (**Figure 2(d)**): the weights of the can and bag were subtracted after the soil dried in order to calculate the soil weight. For the soil samples which were oven dried, the oven temperature was set to 105°C and the soil samples were dried for 24 hours within their containers (cans or bags).

On the first day of sampling, we carefully chose locations with different SWC conditions based on the wetness of the soil. The sampling dates were also carefully chosen between May to July 2019. In order to obtain the wettest SWC value, we consistently measured SWC after storm events, using all 16 SWC probes and the wettest sampling locations. Every one or two days after a storm event, we conducted sampling at around 8 a.m., and 5 p.m. to obtain drier and drier SWC conditions than those taken immediately after the storm event. We did not collect soil samples during storm events; all data was collected during drying cycles. **Figure**

4 illustrates the SCAN site Powder Mill (2049) hourly SWC time series with a hyetograph during the experiment period. The red dots indicate sampling dates. On each sampling date, certain of the thirty locations shown in **Figure 1(a)** were selected for sampling based on soil wetness conditions. For instance, if a location had drier SWC values on a new sampling date than on a previous sampling date, we chose that location for sampling to ensure that we collected the drier SWC values. For a selected sampling location, all 16 probes were used to measure SWC, and soil samples were taken. Each sampling location was visited at least three times during the study period. This process allowed us to obtain the wettest to driest (or near-driest) possible ranges of SWC in the sandy loam areas of the OPE3 site.

The linear regression equations were determined by comparing the GVWC values (θ_{GVWC}), and the SWC values were estimated with the sensors (θ_{sensor}). Before and after site-specific calibration, the corresponding error statistics were calculated.

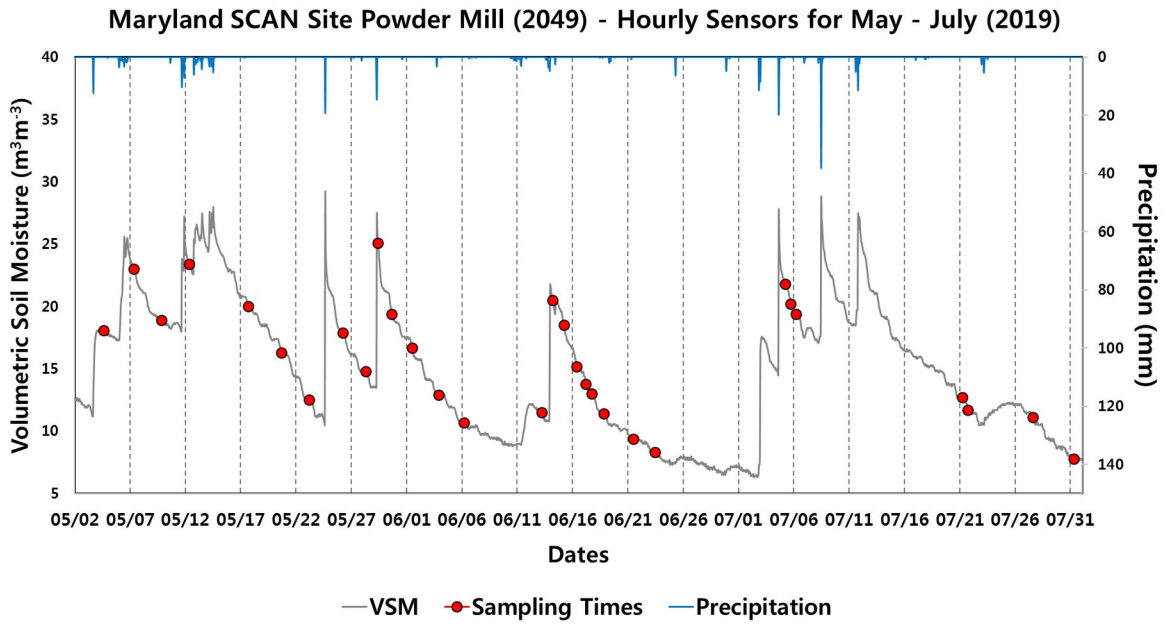

Figure 4. The hourly SWC (at 5-cm depth) time series and hyetograph during the study

period in SCAN site Powder Mill. The sampling dates are indicated with red dots.

4.3 Statistical Metrics

For all sensors, we considered four statistical indicators: R-value, (Eq. (2a)), bias (Eq. (2b)), root mean square difference (RMSD), and unbiased root mean square difference (ubRMSD, Eq. (2c)) (where additive bias had been removed) were calculated when the p-value was below 0.05.

$$R = \frac{cov\left(\theta_{REF}, \theta_{sensor}\right)}{std\left(\theta_{GVWC}\right) std\left(\theta_{sensor}\right)} [2a]$$

$$bias = \frac{\sum_{i=1}^{N} \left(\theta_{sensor_i} - \theta_{GVWCF_i}\right)}{N} [2b]$$

$$RMSD = \sqrt{\frac{\sum_{i=1}^{N} \left(\theta_{GVWC_i} - \theta_{sensor_i}\right)^2}{N}} [2c]$$

$$ubRMSD = \sqrt{\frac{\sum_{i=1}^{N} \left[\left(\theta_{GVWC_i} - \frac{\sum_{i=1}^{N} \theta_{GVWC_i}}{N}\right) - \left(\theta_{sensor_i} - \frac{\sum_{i=1}^{N} \theta_{sensor_i}}{N}\right)\right]^2}{N}} [2d]$$

Where $cov(\cdot)$ and $std(\cdot)$ calculate covariance and standard deviation statistics and N is 30. Positive or negative bias values indicate overestimation or underestimation of SWC from SWC probes. We also considered ubRMSD as the variability of ρ_b of the soils can cause large variance in θ_{GVWC}, thus introducing systematic errors.

4.4 Two-Sample *t*-test and Kolmogorov-Smirnov test

In order to determine whether the different types of portable SWC sensors of similar electrode length showed similar performance, we conducted a two-sample *t*-test ($\alpha = 0.01$). A two-sample *t*-test is used to test the hypothesis of equality between two population means, assuming that the populations exhibit similar means (Kirkwood and Sterne, 2010). Prior to conducting a two-sample *t*-test, the population of the dataset must be verified. The two populations are assumed to be normally distributed based on a Kolmogorov-Smirnov test ($\alpha = 0.01$).

4.5 Maximize R Method

The linear correction method described in section 4.2, corrects for a known portion of systematic error in the data measured from the portable sensors. Thus, after site-specific calibration of the data based on the linear correction method, the corrected VWC data will have no systematic errors. However, this linear correction method will not improve the R- and ubRMSD values.

The maximize R method is a weighted linear combination method for combining two individual data sets; it is a physics-based data fusion method introduced by Kim et al. (2015). This method produces combined data from parent data sets. The combined data will always have an improved R-values compared to the parent data sets. Previous research has shown that a combined product based on the maximize R method is always superior to the combined data sets of an individual product (Kim et al., 2018; Baik et al., 2018).

In this study, we introduced an application of the maximize R method which combines the VWC data from two different types of sensors (i.e., parent datasets) to obtain improved

362 temporal variation. Using this methodology, we produced VWC data of a higher correlation
363 with the GVWC data. Since GVWC is the target value which EM-based probes seek to
364 estimate, obtaining VWC data having close temporal correlation with GVWC data is
365 significant. As we mentioned earlier, the linear correction method cannot improve the R-
366 value, but the maximize R method can improve it.

367 **Figure 5** shows a schematic step-by-step diagram of the maximize R method. The three steps
368 of the detailed description are as follows:

369 • **Step 1**: Two different types of sensors must be inserted closely, either vertically (Type 1 as
370 shown in **Figure 5, Step 1**) or horizontally (Type 2 as shown in **Figure 5, Step 1**). For
371 vertical installation, the two sensor types must have similar electrode lengths in order to
372 measure VWC at similar soil depths. On the other hand, for horizontal installation (Type 2),
373 two different sensor types can have different electrode lengths because they will measure
374 VWC at similar depths. For satellite-based SWC validation field campaigns, sensor
375 installation normally follows Type 1; but for long-term monitoring of VWC, sensor
376 installation normally follows Type 2.

377 • **Step 2**: It is important to collect VWC data simultaneously from two different types of
378 sensors. For Type 1, while the probes are measuring VWC, soil samples for GVWC
379 calculation should be taken from a depth similar to the sensors' electrode lengths. For Type 2,
380 while the probes are measuring VWC, soil samples for GVWC calculation should be taken
381 from the same depths where the two sensors are buried. This GVWC data is the target data
382 that we want to estimate from two different types of sensors.

383 • **Step 3**: After collecting sufficient data from Step 2, we can combine the VWC measured

384 from two different type of sensor using Eqs. 3[a] - 3[d], shown below.

385

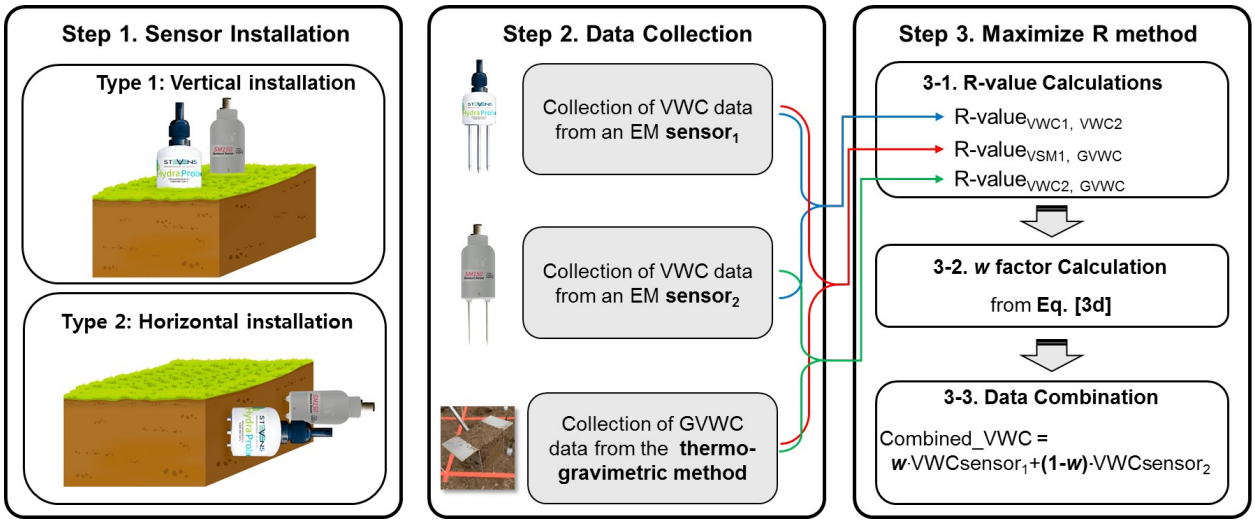

386

387 **Figure 5** A step-by-step schematic diagram of the maximize R method. VWC data are
388 measured from two different types of sensors by inserting them vertically or horizontally
389 (Step 1). VWC data should be collected simultaneously from two different types of sensors
390 and from the thermo-gravimetric method (Step 2). These collected data are then used to
391 calculate the w factor, which will be used to combine the VWC data collected from two
392 different types of sensors (Step 3).

393 In the present study, all EM-based SWC probes inserted
394 perpendicularly into the soil surface (shown described as Type 1) as are
395 shown in Figure 5, Step 1. Thus, only the VWC measured in the similar
396 depth of soil (top 5 to 6 cm) by the ML3, HydraProbe, and SM150 sensors
397 in similar depths of soil (top 5 to 6 cm) are were only considered for the
398 maximize R method for in this study.

399 Two sets of VWC measurements from two different types of sensors were combined into

400 combined VWC values (θ_C) by applying a weighting factor (w) with a constrained range of 0
401 to 1 as follows:

402

403 $$\theta_{C_{(sensor\,1,sensor\,2)}} = w \times \theta_{sensor_1} + (1-w) \times \theta_{sensor_2} (0 \le w \le 1) [3a]$$

404

405 In order to determine the optimum w value that maximizes the R-value between θ_C and θ_{GVWC},
406 it is necessary to express the R-value as a function of θ_C and θ_{GVWC} as follows:

407

408 $$R = f(w) = \frac{E[(\theta_C - \mu_{\theta_C})(\theta_{GVWC} - \mu_{\theta_{GVWC}})]}{\sigma_{\theta_C} \sigma_{\theta_{GVWC}}} [3b]$$

409

410 Where μ stands for the average and σ stands for the standard deviation of each datum. Before
411 combining the two different SWC measurements in Eq. [3a], the systematic differences
412 between θ_{GVWC} and each VWC datasets measured by an EM-based SWC probe must be
413 removed. Previously, Draper et al. (2012) suggested a method to normalize each VWC
414 measurement against the reference data (e.g., GVWC) using Eq. [3c]:

415

416 $$\theta_{NORM} = (\theta_{sensor} - \mu_{\theta_{sensor}}) \times \frac{\sigma_{\theta_{GVWC}}}{\sigma_{\theta_{sensor}}} + \mu_{\theta_{GVWC}} [3c]$$

417

418 Eq. [3b] can be differentiated with regard to w, and the resulting w value should theoretically
419 maximize the R-value between θ_C and θ_{GVSM}. After the differentiation of Eq. [3b], w is

expressed as a function of the R-values between VWC measured from each EM-based SWC probe and GVWC dataset as follows:

$$w = \frac{R_{sensor_1 \cdot GVWC} - R_{sensor_1 \cdot sensor_2} \times R_{sensor_2 \cdot GVWC}}{\left(R_{sensor_2 \cdot GVWC} - R_{sensor_1 \cdot sensor_2} \times R_{sensor_1 \cdot GVWC}\right) + \left(R¿¿sensor_1 \cdot GVWC - R_{sensor_1 \cdot sensor_2} \times R_{sensor_2 \cdot GVWC}\right)[3d]¿}$$

where $R_{x\text{-}y}$ is the R-value between two individual measurements after removing systematic differences, according to Eq. [3c].

In order to obtain an unbiased *w* factor, VWC data of all possible ranges within the area of interest should be collected. In addition, to determine the *w* factors, a large enough sample size of GVWC and VWC from two different types of sensors is required in order to calculate the robust statistics shown in Eqs. 3[a] - 3[d].

5 Results and Discussion

5.1 Results of Site-specific Correction

The results of default factory-calibration SWC data are illustrated in **Figure 6** using linear regression. All statistical numbers, including the bias (m^3m^{-3}), RSMD (m^3m^{-3}), ubRMSD (m^3m^{-3}), R-value, and constants in linear regression (i.e., *m* and *n*) lines, are shown in **Table 3**. Since the target accuracy of the SMAP satellite mission is ±0.04 m^3m^{-3} (Entekhabi et al., 2010), the RMSD of the SWC probes should be at or below this magnitude in order to validate the satellite-based SWC estimates. In **Figure 6** and **Table 3**, with SWC data estimated using the manufacturer's calibration, some SWC probes had RMSD values higher

441 than 0.04 m^3m^{-3}; however, all three ML3s, HydraProbe(B),all three SM150s, and the PICO64
442 had RMSD values lower than 0.04 m^3m^{-3}.

443 Huang et al. (2004) also reported RMSD values of 0.037 m^3m^{-3} for ML3s and concluded
444 that ML3s were more accurate than other soil water instruments (Watermark, Aquaterr, and
445 Aqua-Tel sensors) in sandy loam soil and required no calibration under laboratory conditions.
446 Furthermore, under laboratory conditions. ML3 RMSD values of 0.020 ~ 0.040 m^3m^{-3} were
447 reported in other literature (Fares et al., 2011; Vaz et al., 2013). Finally, in our study, the ML#
448 ubRMSD values obtained in field conditions were close to the reported laboratory accuracy
449 of 0.020 m^3m^{-3} (Vaz et al., 2013). The HydraProbe showed an average RMSD value of 0.044
450 m^3m^{-3}, but HydraProbe(A) and (C) showed relatively higher RMSD values: 0.050 m^3m^{-3} and
451 0.052 m^3m^{-3}. Seyfried and Murdock (2004) noted that for the HydraProbe, the factory
452 calibration function for a generic soil has an RMSD of 0.330 m^3m^{-3} due to the limited
453 dielectric range imposed by the unrealistic shape of its calibration function. Considering that
454 10% of our GVWC data is higher than 0.330 m^3m^{-3}, the relatively high RMSD might be
455 caused by a SM range which was higher than 0.330 m^3m^{-3} during the study period.
456 Furthermore, the RMSD and ubRMSD of the SM150 sensors are lower than those of all other
457 sensors except the PICO64. In terms of RMSD, the SM150 using the factory default
458 calibration performs better than other sensors of similar sensing depths (the ML3 and HP
459 probes) (**Table 3**). The RMSD values for the default factory and site-specific correction
460 measurements were 0.028 m^3m^{-3} and 0.021 m^3m^{-3}, respectively. Furthermore, Zhu et al.
461 (2019) reported that the SM150 produced the highest accuracy of all TLO- and FDR-type
462 sensors in silt loam. However, the permittivity of the soil could cause an anomaly in the
463 transmitted EM field since the EM field is affected by other soil properties. Therefore, in
464 other soil conditions, the performance of SM150 may vary.

After site-specific correction, the ubRMSD values from three probes of similar sensing depths, the ML3s, HydraProbes, and SM150s were almost identical: 0.020 m^3m^{-3}, 0.023 m^3m^{-3}, and 0.020 m^3m^{-3}, respectively. For ML3 sensors, after site-specific correction, the average RMSD value decreased from 0.035 m^3m^{-3} to 0.021 m^3m^{-3}. However, Cosh et al. (2005) reported that after field-specific calibration for soil type of sandy loam/sand (sand range 0-25% and clay range 50-70%), ML2 sensors used in measuring 21 field samples returned an RMSD of 0.043 m^3m^{-3}. Since Vaz et al. (2013) reported a lower performance of ML3 sensors in soil with high fractions of clay than in sandy soils, the lower RMSE results produced by the current research may be the result of the soil type, which were composed mostly of sandy loam. Fares et al. (2011) reported an RMSE value of 0.019 m^3m^{-3} after applying the calibration function to the ML3 laboratory calibration equations. These results indicate that for collecting SWC data at shallow soil depths (0-5 cm) for remotely-sensed SWC data, the ML3, HydraProbe, and SM150--along with portable devices--are suitable for sandy loam soil conditions after site-specific correction.

Of all the sensors studied, the PICO64, which is based on the principle of TLO, showed excellent performance both before and after site-specific correction: the ubRMSD values were 0.017 m^3m^{-3} before site-specific correction and 0.016 m^3m^{-3} after site-specific correction. The PICO64 probe is less susceptible to interference from EC because it operates at a high frequency (1,000 MHz) than capacitance probes (Robinson et al., 2008). High frequencies, such as 1,000 MHz, can carry out an exact partition of moisture and conductivity, unlike capacitive probes with lower frequencies. This difference in performances is due to the fact that capacitance probes are affected by the EC properties of soil. Of all the sensors, the FS100 showed the greatest improvement after site-specific correction: all FS100s produced RMSD values lower than 0.02 m^3m^{-3}. The average statistics from all the FS100s showed the highest

R-value (average 0.959) and the lowest ubRMSD (average 0.015 m^3m^{-3}) after site-specific correction. There appeared to be a large improvement (0.037 m^3m^{-3}) in the RMSD of the FS100s after correction, dropping from 0.052 before correction to 0.015 m^3m^{-3} afterward. Site-specific correction decreased RMSD errors of all FS100 sensors to less than 0.02 m^3m^{-3} with negligible bias. This result indicates that after proper correction, all portable sensors tested in the present work can be utilized to validate satellite-based SM estimates with good accuracy (better than ±0.04 m^3m^{-3}). However, site-specific correction is always recommended before beginning a validation effort or a field campaign. This result also indicates that several separate calibration efforts may be required to accurately represent satellite-based SM estimates over large areas (i.e., several kilometers) with multiple soil types.

Table 3. Summary statistics for the default factory calibration and site-specific correction of each SM probe.

	Default Factory Calibration		Site-specific Correction				Correction Eq.	
Probes	**bias**	**RMSD**	**bias**	**RMSD**	**ubRMSD**	**R-value**	**Slope** m	**y-intercept** n
ML3(A)	-0.026	0.033	0.000	0.022	0.021	0.920	0.976	0.031
ML3(B)	-0.033	0.039	0.000	0.021	0.020	0.926	0.960	0.042
ML3(C)	-0.027	0.033	0.000	0.019	0.018	0.941	1.058	0.015
AVG.	-0.029	0.035	0.000	0.021	0.020	0.929		
HydraProbe(A)	-0.042	0.050	0.000	0.026	0.025	0.883	0.812	0.080
HydraProbe(B)	-0.019	0.030	0.000	0.022	0.021	0.917	0.843	0.054
HydraProbe(C)	-0.047	0.052	0.000	0.022	0.021	0.918	0.940	0.059
AVG.	-0.036	0.044	0.000	0.023	0.023	0.906		
SM150(A)	-0.018	0.028	0.000	0.019	0.019	0.937	0.850	0.052
SM150(B)	-0.016	0.028	0.000	0.022	0.022	0.916	0.839	0.053
SM150(C)	-0.019	0.030	0.000	0.021	0.021	0.923	0.855	0.052
AVG.	-0.018	0.028	0.000	0.021	0.020	0.926		
HS2(A)	-0.058	0.063	0.000	0.025	0.025	0.887	0.972	0.063
HS2(B)	-0.049	0.054	0.000	0.023	0.022	0.914	1.070	0.035
HS2(C)	-0.058	0.062	0.000	0.023	0.022	0.913	1.002	0.058
AVG.	-0.055	0.059	0.000	0.024	0.023	0.905		
FS100(A)	-0.044	0.047	0.000	0.018	0.017	0.947	0.927	0.058
FS100(B)	-0.058	0.059	0.000	0.012	0.011	0.977	0.966	0.064
FS100(C)	-0.046	0.049	0.000	0.017	0.016	0.952	0.985	0.049
AVG.	-0.049	0.052	0.000	0.015	0.015	0.959		
PICO64	0.014	0.022	0.000	0.017	0.016	0.942	1.105	-0.041

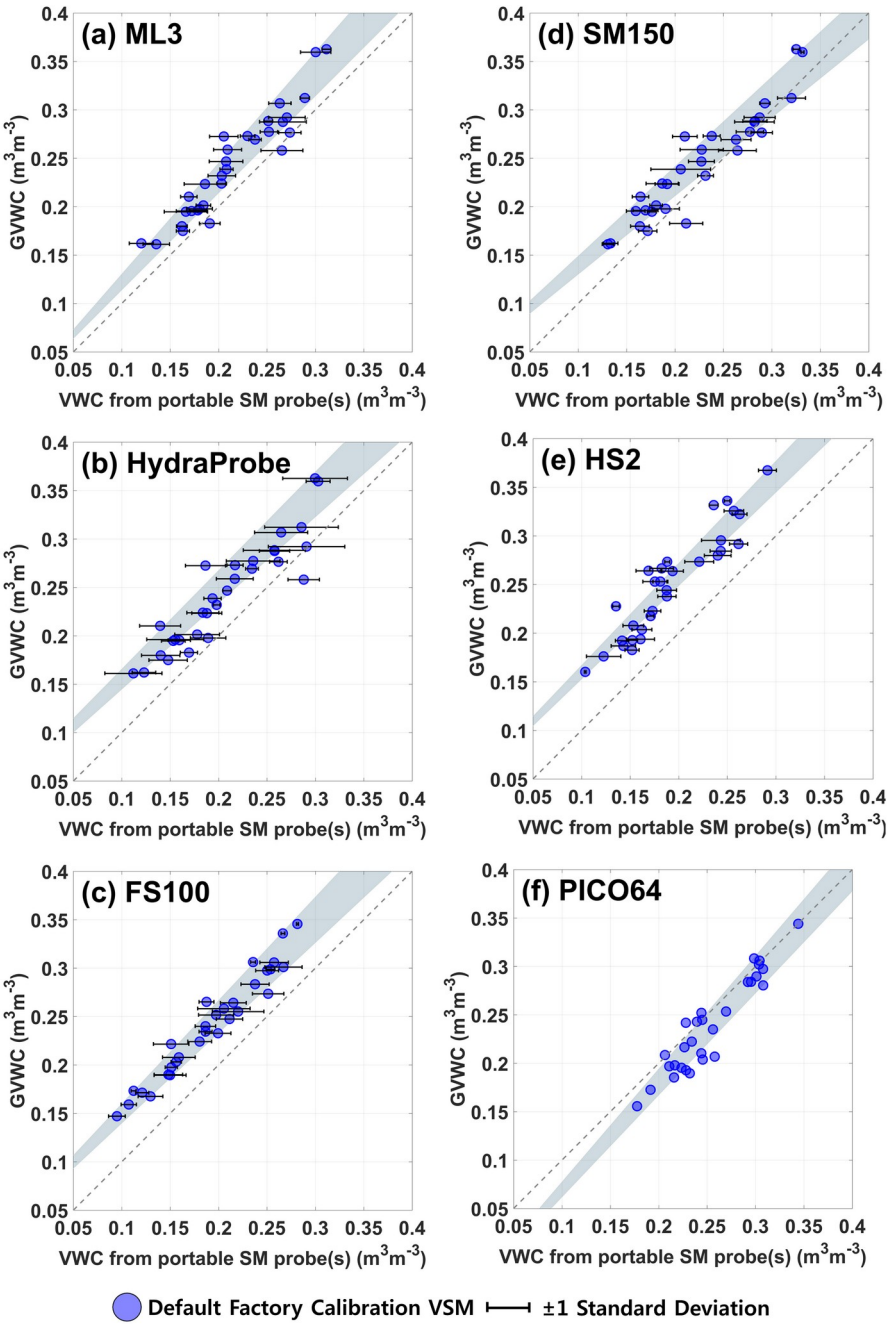

Figure 6. Factory calibrated VWC from physical sampling versus the paired mean of 3 sensors for (a) ML3, (b) HydraProbe, (c) FS100, (d) SM150, (e) HS2, and 1 sensor value for (f) PICO64. The gray shaded areas in the scatter plots are the possible correction lines from different ρ_b values of 0-5 cm depth at the OPE3 site and horizontal error bars indicate the standard deviation of paired data sets.

508 **5.2. Results of two-sample *t*-test**

509 The null hypothesis of the two-sample *t*-test is that the data in a pair of SWC
510 measurements from sensors come from normal distributions with the same mean. A p-value
511 with a significance level of less than 1% rejects the null hypothesis. **Figure S1** shows the p-
512 value results of two-sample *t*-test for sensors of similar electrode lengths (5-6 cm), including
513 ML3s, HydraProbes, and SM150s. We did not perform two-sample *t*-test on variances pairing
514 the CS659 and the FS100 with other sensors because the CS659 and FS100's electrode
515 lengths are quite different from those of the ML3s, HydraProbes, and FS100s. Furthermore,
516 since only one PCIO64 was tested in this study, no two-sample *t*-test was conducted for this
517 type of sensor.

518 In **Figure S1**, it is observed when the manufacturer's calibration is used to estimates
519 SWC sensors having similar electrode lengths (e.g., ML3 vs. HS, ML3 vs. SM150, and HS
520 vs. SM150) the null hypothesis of two-sample *t*-test was not rejected. This is because the
521 SWC measurements from sensors of similar electrode lengths were statistically similar
522 without site specific correction.

523

524 **5.3 Results of combined VWC data calculated from two different types of EM-based**
525 **probes**

526 **Tables 4** shows the improvement in R-value after combining two different types of
527 sensors for the 0-5 cm SWC estimations (ML3, HydraProbe, and SM150). The results show
528 that the R-value is always higher after combining data from two different types of sensors.
529 The maximum improvements in R-value were found when the HydraProbe sensors were used
530 with ML3 sensors. Specifically, the R-value for single-sensor use of HydraProbe(A)

improved from 0.883 to 0.941 when HydraProbe(A) was combined with ML3(C) (**Table 4**). On average, when any two sensors were combined, the R-value increased by about 1.9%; and the maximum improvement in R-value was about 2.8% (*Improvement (%) in R-value* column in **Tables 4**). The average R-value improved from 0.930 to 0.959.

Tables 5 shows the *w* factor for each pair of sensors for 0-5 cm depths of SWC data. The largest *w* factor is shown in the ML3(C) (0.747; the ML3(C) row and the *AVG.* column in **Table 5**), and the average *w* factor for all ML3 sensors was 0.625 (*Same sensor type AVG.* column in **Table 5**). This result indicates that the ML3 sensor is the major contributor in improving the R-value of data combinations measuring 0-5 cm SWC.

Before combination of two different SWC measurements from Eq. [3a], the systematic differences between θ_{GVWC} and each parent product were removed. Thus, the RMSD from a single sensor measurement decreased dramatically. **Tables 6** shows the results of RSMD before and after the two different types of sensors were paired. The greatest improvement in RMSD was shown when the HydraProbe was combined with the ML3. On average, when a sensor of one type was combined with a sensor of another type, the RMSD decreased by about 44.8% of the original error. The average maximum decrease in RMSD was 47.5% (*Improvement (%) in RMSD* column in **Table 6**). The average RMSD decreased from 0.036 m^3m^{-3} to 0.018 m^3m^{-3}.

In this study, we proposed combining two different types of EM-based SM probes to improve the quality of SM data. However, it is worth noting that the currently determined *w* factors shown in this study are not applicable to other soil properties because these values were determined only for sandy loam and only for one specific depth of soil (0-5 cm). Although the proposed method can improve R and ubRMSD statistics, for practical application, *w* factors should be determined for each study area of interest.

555 **Table 4**. R-values for ML3, HydraProbe, and SM150 sensors 0-5 cm SM data when combined with a different type of sensor to create sensor
556 paired data.

Sensor	Single sensor R-value	Two sensor combined R-value									Improvement (%) in R-value		
		with ML3(A)	with ML3(B)	with ML3(C)	with Hydra Probe(A)	with Hydra Probe(B)	with Hydra Probe(C)	with SM150(A)	with SM150(B)	with SM150(C)	AVG.	Maximum	Same sensor type AVG.
ML3(A)	0.920	-	-	-	0.921	0.933	0.934	0.943	0.939	0.941	1.6	2.4	**ML3**
ML3(B)	0.926	-	-	-	0.927	0.938	0.938	0.947	0.932	0.939	1.2	2.3	1.8
ML3(C)	0.941	-	-	-	0.941	0.946	0.947	0.948	0.942	0.945	0.4	0.7	
Hydra Probe(A)	0.883	0.921	0.927	0.941	-	-	-	0.937	0.919	0.926	5.2	6.6	**HydraProbe**
Hydra Probe(B)	0.917	0.933	0.938	0.946	-	-	-	0.944	0.934	0.943	2.5	3.2	4.9
Hydra Probe(C)	0.918	0.934	0.938	0.947	-	-	-	0.944	0.932	0.932	2.2	3.1	
SM150(A)	0.937	0.943	0.947	0.948	0.937	0.944	0.944	-	-	-	0.7	1.2	**SM150**
SM150(B)	0.916	0.939	0.932	0.942	0.919	0.934	0.932	-	-	-	1.9	2.9	2.1
SM150(C)	0.923	0.941	0.939	0.945	0.926	0.943	0.932	-	-	-	1.6	2.3	
										AVG.	1.9	2.8	

557 **Table 5**. ML3, HydraProbe, and SM150 weighting factor (w) to combine different pairs of SM measurements for 0-5 cm depth.

558

		Optimized Weighting Factor (w) (combined_data = w*Data_1+(w-1)*Data_2)										
		Data_2										
	Sensor	**with ML3(A)**	**with ML3(B)**	**with ML3(C)**	**with HydraProbe(A)**	**with HydraProbe(B)**	**with HydraProbe(C)**	**with SM150(A)**	**with SM150(B)**	**with SM150(C)**	**AVG.**	**Same sensor type AVG.**
Data_1	**ML3(A)**	-	-	-	0.892	0.531	0.520	0.334	0.527	0.482	0.548	**ML3**
	ML3(B)	-	-	-	0.832	0.565	0.560	0.403	0.611	0.521	0.582	0.625
	ML3(C)	-	-	-	0.993	0.699	0.692	0.553	0.833	0.709	0.747	
	HydraProbe(A)	0.108	0.168	0.007	-	-	-	0.002	0.233	0.216	0.150	**HydraProbe**
	HydraProbe(B)	0.469	0.435	0.301	-	-	-	0.334	0.506	0.465	0.435	0.339
	HydraProbe(C)	0.480	0.440	0.308	-	-	-	0.337	0.516	0.441	0.432	
	SM150(A)	0.666	0.597	0.447	0.998	0.666	0.663	-	-	-	0.775	**SM150**
	SM150(B)	0.473	0.389	0.167	0.767	0.494	0.484	-	-	-	0.582	0.661
	SM150(C)	0.518	0.479	0.291	0.784	0.535	0.559	-	-	-	0.626	

559 **Table 6.** ML3, HydraProbe, and SM150 RMSD after combining different pairs of SM measurements for 0-5 cm depth.

560

Sensor	Single sensor RMSD (m3/m3)	Two sensors combined RMSD									Improvement (%) in RMSD		
		with ML3(A)	with ML3(B)	with ML3(C)	with HydraProbe(A)	with HydraProbe(B)	with HydraProbe(C)	with SM150(A)	with SM150(B)	with SM150(C)	AVG.	Maximum	Same sensor type AVG.
ML3(A)	0.033	-	-	-	0.021	0.020	0.019	0.018	0.019	0.018	-42.3	-36.0	**ML3**
ML3(B)	0.039	-	-	-	0.020	0.019	0.019	0.017	0.020	0.019	-51.3	-47.6	-42.4
ML3(C)	0.033	-	-	-	0.018	0.017	0.017	0.017	0.018	0.018	-45.7	-43.6	
HydraProbe(A)	0.050	0.021	0.020	0.018	-	-	-	0.019	0.021	0.020	-59.9	-63.3	**HydraProbe**
HydraProbe(B)	0.030	0.020	0.019	0.017	-	-	-	0.018	0.019	0.018	-37.9	-43.8	-53.6
HydraProbe(C)	0.052	0.019	0.019	0.017	-	-	-	0.018	0.020	0.020	-63.7	-65.4	
SM150(A)	0.027	0.018	0.017	0.017	0.019	0.018	0.018	-	-	-	-34.9	-44.3	**SM150**
SM150(B)	0.028	0.019	0.020	0.018	0.021	0.019	0.020	-	-	-	-30.9	-39.3	-42.5
SM150(C)	0.030	0.018	0.019	0.018	0.020	0.018	0.020	-	-	-	-36.3	-43.9	
										AVG.	-44.8	-47.5	

561 **6 Conclusion**

562 We compared, corrected, and combined 6 commonly used and/or newly available
563 portable EM-based SWC probes equipped with portable data loggers. Our first finding was
564 that without site-specific correction, some of the portable EM-based SWC probes, including
565 the HydraProbe, HS2, and FS100 sensors, showed RMSD values greater than 0.040 m^3m^{-3}
566 (accuracy required by SMAP soil moisture products). In other words, they demonstrated
567 unsatisfactory accuracy for validating remotely sensed SWC data in sandy loam soils.
568 However, after site-specific correction, the RMSD for all sensors decreased to less than 0.025
569 m^3m^{-3}. These results indicate that SWC probes with portable devices are suitable for
570 validating large-scale SWC estimates in a sandy loam soil, after implementation of site-
571 specific correction. Use of portable EM-based SWC probes presents a quick and easy way to
572 take multiple observations within various satellite pixels – either at the original resolution
573 (e.g., ~36-km products from SMAP and SMOS product) or at the downscaled resolution of
574 SWC products (e.g., 1-km products from SMAP/Sentinel or Sentinel-1). The accuracy of the
575 portable EM-based SWC probes is greater than the requirements for satellite soil moisture
576 retrievals makes these probes a very attractive option for future validation studies. However,
577 it should be noted that we have undertaken this evaluation at the OPE3 site with sandy loam
578 soils. Therefore, results shown in this study are only valid for similar soil properties because
579 capacitance and quasi-TDR sensors are influenced by EC and soil texture and cannot be
580 generalized to other locations with soils types other than sandy loam.

581 Second, we conducted two-sample *t*-test to determine whether VWC data measured from
582 the different types of sensors showed significantly similar performance. The two-sample *t*-
583 test results showed that VWC measurements from EM-based SWC probes of similar
584 electrode lengths were statistically similar without site-specific correction.

Third, using the Maximize R method, we combined VWC data from different pairs of VWC sensors. Data combination greatly improved the R-values and decreased the ubRMSD. These results suggest that, in addition to performing site-specific correction, EM-based SWC probes can be used in pairs to produce more accurate VWC data and reduce the systematic bias of VWC sensors.

Acknowledgments

We gratefully acknowledge funding from the NASA Terrestrial Hydrology Program (Program Manager Dr. Jared Entin, Grant #NNX12AP75G). Hyunglok Kim acknowledges the Future Investigators in NASA Earth and Space Science and Technology (FINESST) Award and the Bicentennial Fellowship from the Department of Engineering Systems and Environment at the University of Virginia. We particularly appreciate Dr. Maheshwari Neelam and Mr. Alex White for their valuable comments. USDA is an equal opportunity employer and provider. This research was a contribution from the Long-Term Agroecosystem Research (LTAR) network. LTAR is supported by the United States Department of Agriculture.

References

Abbas, F., A. Fares, and S. Fares. 2011. Field Calibrations of Soil Moisture Sensors in a Forested Watershed. Sensors 11(6): 6354–6369. doi: 10.3390/s110606354.

Bai, X., B. He, and X. Li. 2016. Optimum Surface Roughness to Parameterize Advanced Integral Equation Model for Soil Moisture Retrieval in Prairie Area Using Radarsat-2 Data. IEEE Trans. Geosci. Remote Sens. 54(4): 2437–2449. doi: 10.1109/TGRS.2015.2501372.

Baik, J., U.W. Liaqat, and M. Choi. 2018. Assessment of satellite- and reanalysis-based evapotranspiration products with two blending approaches over the complex landscapes and climates of Australia. Agric. For. Meteorol. 263: 388–398. doi: 10.1016/j.agrformet.2018.09.007.

Benor, M., G.J. Levy, Y. Mishael, and A. Nadler. 2013. Salinity Effects on the Fieldscout TDR 300 Soil Moisture Meter Readings. Soil Sci. Soc. Am. J. 77(2): 412–416. doi: 10.2136/sssaj2012.0294n.

Birchak, J.R., C.G. Gardner, J.E. Hipp, and J.M. Victor. 1974. High dielectric constant microwave probes for sensing soil moisture. Proc. IEEE 62(1): 93–98. doi: 10.1109/PROC.1974.9388.

Blonquist, J.M., S.B. Jones, and D.A. Robinson. 2005. Standardizing Characterization of Electromagnetic Water Content Sensors. Vadose Zone J. 4(4): 1059–1069. doi: 10.2136/vzj2004.0141.

Bosch, D.D. 2004. Comparison of Capacitance-Based Soil Water Probes in Coastal Plain Soils. VADOSE ZONE J 3: 10.

Bosch, D.D., V. Lakshmi, T.J. Jackson, M. Choi, and J.M. Jacobs. 2006. Large scale measurements of soil moisture for validation of remotely sensed data: Georgia soil moisture experiment of 2003. J. Hydrol. 323(1): 120–137. doi: 10.1016/j.jhydrol.2005.08.024.

Caldwell, T.G., T. Bongiovanni, M.H. Cosh, C. Halley, and M.H. Young. 2018. Field and Laboratory Evaluation of the CS655 Soil Water Content Sensor. Vadose Zone J. 17(1): 170214. doi: 10.2136/vzj2017.12.0214.

Caldwell, T.G., T. Bongiovanni, M.H. Cosh, T.J. Jackson, A. Colliander, et al. 2019. The Texas Soil Observation Network:A Comprehensive Soil Moisture Dataset for Remote Sensing and Land Surface Model Validation. Vadose Zone J. 18(1): 0. doi: 10.2136/vzj2019.04.0034.

Cassel, D.K., R.G. Kachanoski, and G.C. Topp. 1994. Practical Considerations for Using A TDR Cable Tester to Measure Soil Water Content. Soil Technol. 7: 113–162.

Chandler, D.G., M. Seyfried, M. Murdock, and J.P. McNamara. 2004. Field Calibration of Water Content Reflectometers. Soil Sci. Soc. Am. J. 68(5): 1501–1507. doi:

638 10.2136/sssaj2004.1501.

639 Chow, L., Z. Xing, H.W. Rees, F. Meng, J. Monteith, et al. 2009. Field performance of nine
640 soil water content sensors on a sandy loam soil in new brunswick, maritime region,
641 Canada. Sensors 9(11): 9398–9413. doi: 10.3390/s91109398.

642 Cosh, M.H., T.J. Jackson, R. Bindlish, J.S. Famiglietti, and D. Ryu. 2005. Calibration of an
643 impedance probe for estimation of surface soil water content over large regions. J.
644 Hydrol. 311(1–4): 49–58. doi: 10.1016/j.jhydrol.2005.01.003.

645 Cosh, M.H., T.J. Jackson, S. Moran, and R. Bindlish. 2008. Temporal persistence and
646 stability of surface soil moisture in a semi-arid watershed. Remote Sens. Environ.
647 112(2): 304–313. doi: 10.1016/j.rse.2007.07.001.

648 Cosh, M.H., T.E. Ochsner, L. McKee, J. Dong, J.B. Basara, et al. 2016. The Soil Moisture
649 Active Passive Marena, Oklahoma, In Situ Sensor Testbed (SMAP-MOISST):
650 Testbed Design and Evaluation of In Situ Sensors. Vadose Zone J. 15(4): 0. doi:
651 10.2136/vzj2015.09.0122.

652 De Lannoy, G.J.M., N.E.C. Verhoest, P.R. Houser, T.J. Gish, and M. Van Meirvenne. 2006.
653 Spatial and temporal characteristics of soil moisture in an intensively monitored
654 agricultural field (OPE3). J. Hydrol. 331(3): 719–730. doi:
655 10.1016/j.jhydrol.2006.06.016.

656 Dettmann, U., and M. Bechtold. 2018. Evaluating Commercial Moisture Probes in Reference
657 Solutions Covering Mineral to Peat Soil Conditions. Vadose Zone J. 17(1): 0. doi:
658 10.2136/vzj2017.12.0208.

659 Draper, C.S., R.H. Reichle, G.J.M. De Lannoy, and Q. Liu. 2012. Assimilation of passive and
660 active microwave soil moisture retrievals: ASCAT AMSR-E ASSIMILATION.
661 Geophys. Res. Lett. 39(4): n/a-n/a. doi: 10.1029/2011GL050655.

662 Dumedah, G., J. P. Walker, and O. Merlin. 2015. Root-zone soil moisture estimation from
663 assimilation of downscaled Soil Moisture and Ocean Salinity data. Adv. Water
664 Resour. 84: 14–22. doi: 10.1016/j.advwatres.2015.07.021.

665 Entekhabi, D., E.G. Njoku, P.E. O'Neill, K.H. Kellogg, W.T. Crow, et al. 2010. The Soil
666 Moisture Active Passive (SMAP) Mission. Proc. IEEE 98(5): 704–716. doi:
667 10.1109/JPROC.2010.2043918.

668 Evett, S.R., J.A. Tolk, and T.A. Howell. 2006. Soil Profile Water Content Determination.
669 Vadose Zone J. 5(3): 894. doi: 10.2136/vzj2005.0149.

670 Fares, A., F. Abbas, D. Maria, and A. Mair. 2011. Improved Calibration Functions of Three
671 Capacitance Probes for the Measurement of Soil Moisture in Tropical Soils. Sensors
672 11(5): 4858–4874. doi: 10.3390/s110504858.

673 Heimovaara, T.J., E.J.G. de Winter, W.K.P. van Loon, and D.C. Esveld. 1996. Frequency-
674 Dependent Dielectric Permittivity from 0 to 1 GHz: Time Domain Reflectometry
675 Measurements Compared with Frequency Domain Network Analyzer Measurements.

676 Water Resour. Res. 32(12): 3603–3610. doi: 10.1029/96WR02695.

677 Hoekstra, P., and A. Delaney. 1974. Dielectric properties of soils at UHF and microwave
678 frequencies. J. Geophys. Res. 1896-1977 79(11): 1699–1708. doi:
679 10.1029/JB079i011p01699.

680 Hottenstein, J.D., G.E. Ponce-Campos, J. Moguel-Yanes, and M.S. Moran. 2015. Impact of
681 Varying Storm Intensity and Consecutive Dry Days on Grassland Soil Moisture. J.
682 Hydrometeorol. 16(1): 106–117. doi: 10.1175/JHM-D-14-0057.1.

683 Huang, Q., O.O. Akinremi, R. Sri Rajan, and P. Bullock. 2004. Laboratory and field
684 evaluation of five soil water sensors. Can. J. Soil Sci. 84(4): 431–438. doi:
685 10.4141/S03-097.

686 Jackson, T., A. Colliander, J. Kimball, R. Reichle, W. Crow, et al. 2012. Science Data
687 Calibration and Validation Plan. : 99.

688 Kargas, G., and P. Kerkides. 2008. Water content determination in mineral and organic
689 porous media by ML2 theta probe. Irrig. Drain. 57(4): 435–449. doi: 10.1002/ird.364.

690 Kelleners, T.J., and J.B. Norto. 2012. Determining Water Retention in Seasonally Frozen
691 Soils Using Hydra Impedance Sensors. Soil Sci. Soc. Am. J. 76(1): 36. doi:
692 10.2136/sssaj2011.0222.

693 Kim, H., R. Parinussa, A.G. Konings, W. Wagner, M.H. Cosh, et al. 2018. Global-scale
694 assessment and combination of SMAP with ASCAT (active) and AMSR2 (passive)
695 soil moisture products. Remote Sens. Environ. 204: 260–275. doi:
696 10.1016/j.rse.2017.10.026.

697 Kim, S., R.M. Parinussa, Yi.Y. Liu, F.M. Johnson, and A. Sharma. 2015. A framework for
698 combining multiple soil moisture retrievals based on maximizing temporal
699 correlation. Geophys. Res. Lett. 42(16): 6662–6670. doi: 10.1002/2015GL064981.

700 Kirkwood, B.R., and J.A.C. Sterne. 2010. Essential Medical Statistics. John Wiley & Sons.

701 Lee, R.K.C., and D.G. Fredlund. 1984. Measurement of Soil Suction Using the MCS 6000
702 Sensor. Fifth Int. Conf. Expans. Soils 1984 Prepr. Pap.: 50.

703 Leib, B.G., J.D. Jabro, and G.R. Matthews. 2003. FIELD EVALUATION AND
704 PERFORMANCE COMPARISON OF SOIL MOISTURE SENSORS: Soil Sci.
705 168(6): 396–408. doi: 10.1097/01.ss.0000075285.87447.86.

706 Lievens, H., S.K. Tomer, A. Al Bitar, G.J.M. De Lannoy, M. Drusch, et al. 2015. SMOS soil
707 moisture assimilation for improved hydrologic simulation in the Murray Darling
708 Basin, Australia. Remote Sens. Environ. 168: 146–162. doi:
709 10.1016/j.rse.2015.06.025.

710 Logsdon, S.D., T.R. Green, M. Seyfried, S.R. Evett, and J. Bonta. 2010. Hydra Probe and
711 Twelve-Wire Probe Comparisons in Fluids and Soil Cores. Soil Sci. Soc. Am. J.
712 74(1): 5. doi: 10.2136/sssaj2009.0189.

713 Magagi, R., A.A. Berg, K. Goita, S. Belair, T.J. Jackson, et al. 2013. Canadian Experiment
714 for Soil Moisture in 2010 (CanEx-SM10): Overview and Preliminary Results. IEEE
715 Trans. Geosci. Remote Sens. 51(1): 347–363. doi: 10.1109/TGRS.2012.2198920.

716 Malicki, M.A., R. Plagge, and C.H. Roth. 1996. Improving the calibration of dielectric TDR
717 soil moisture determination taking into account the solid soil. Eur. J. Soil Sci. 47(3):
718 357–366. doi: 10.1111/j.1365-2389.1996.tb01409.x.

719 Mladenova, I., V. Lakshmi, T.J. Jackson, J.P. Walker, O. Merlin, et al. 2011. Validation of
720 AMSR-E soil moisture using L-band airborne radiometer data from National Airborne
721 Field Experiment 2006. Remote Sens. Environ. 115(8): 2096–2103. doi:
722 10.1016/j.rse.2011.04.011.

723 Moller, J., N. Jovanovic, C.L. Garcia, R.D. Bugan, and D. Mazvimavi. 2018. Validation and
724 downscaling of Advanced Scatterometer (ASCAT) soil moisture using ground
725 measurements in the Western Cape, South Africa. South Afr. J. Plant Soil 35(1): 9–
726 22. doi: 10.1080/02571862.2017.1318962.

727 Morrison, T.A., R.M. Holdo, D.M. Rugemalila, M. Nzunda, and T.M. Anderson. 2019. Grass
728 competition overwhelms effects of herbivores and precipitation on early tree
729 establishment in Serengeti. J. Ecol. 107(1): 216–228. doi: 10.1111/1365-2745.13010.

730 Ponizovsky, A.A., S.M. Chudinova, and Y.A. Pachepsky. 1999. Performance of TDR
731 calibration models as affected by soil texture. J. Hydrol. 218(1): 35–43. doi: 10.1016/
732 S0022-1694(99)00017-7.

733 Reynolds, S.G. 1970. The gravimetric method of soil moisture determination Part I A study
734 of equipment, and methodological problems. J. Hydrol. 11(3): 258–273. doi:
735 10.1016/0022-1694(70)90066-1.

736 Robinson, D.A., C.S. Campbell, J.W. Hopmans, B.K. Hornbuckle, S.B. Jones, et al. 2008.
737 Soil Moisture Measurement for Ecological and Hydrological Watershed-Scale
738 Observatories: A Review. Vadose Zone J. 7(1): 358. doi: 10.2136/vzj2007.0143.

739 Robinson, D.A., S.B. Jones, J.M. Wraith, D. Or, and S.P. Friedman. 2003. A Review of
740 Advances in Dielectric and Electrical Conductivity Measurement in Soils Using Time
741 Domain Reflectometry. Vadose Zone J. 2(4): 444–475. doi: 10.2113/2.4.444.

742 Roets, N.J.R., R.B. Cronje, S.P. Schoeman, N.R. Murovhi, and I.M. Ratlapane. 2013.
743 Calibrating avocado irrigation through the use of continuous soil moisture monitoring
744 and plant physiological parameters. : 6.

745 Roth, K., R. Schulin, H. Flühler, and W. Attinger. 1990. Calibration of time domain
746 reflectometry for water content measurement using a composite dielectric approach.
747 Water Resour. Res. 26(10): 2267–2273. doi: 10.1029/WR026i010p02267.

748 Rowlandson, T.L., A.A. Berg, P.R. Bullock, E.R. Ojo, H. McNairn, et al. 2013. Evaluation of
749 several calibration procedures for a portable soil moisture sensor. J. Hydrol. 498:
750 335–344. doi: 10.1016/j.jhydrol.2013.05.021.

751 Sanchez, N., J. Martinez-Fernandez, A. Scaini, and C. Perez-Gutierrez. 2012. Validation of
752 the SMOS L2 Soil Moisture Data in the REMEDHUS Network (Spain). IEEE Trans.
753 Geosci. Remote Sens. 50(5): 1602–1611. doi: 10.1109/TGRS.2012.2186971.

754 Seyfried, M.S., L.E. Grant, E. Du, and K. Humes. 2005. Dielectric Loss and Calibration of
755 the Hydra Probe Soil Water Sensor. Vadose Zone J. 4(4): 1070–1079. doi:
756 10.2136/vzj2004.0148.

757 Seyfried, M.S., and M.D. Murdock. 2004. Measurement of Soil Water Content with a 50-
758 MHz Soil Dielectric Sensor. SOIL SCI SOC AM J 68: 10.

759 Singh, J., T. Lo, D.R. Rudnick, T.J. Dorr, C.A. Burr, et al. 2018. Performance assessment of
760 factory and field calibrations for electromagnetic sensors in a loam soil. Agric. Water
761 Manag. 196: 87–98. doi: 10.1016/j.agwat.2017.10.020.

762 Smith-Rose, R.L. 1935. The electrical properties of soil at frequencies up to 100 megacycles
763 per second$\mathsemicolon$ with a note on the resistivity of ground in the United
764 Kingdom. Proc. Phys. Soc. 47(5): 923–931. doi: 10.1088/0959-5309/47/5/318.

765 Srivastava, P.K., P. O'Neill, M. Cosh, M. Kurum, R. Lang, et al. 2015. Evaluation of
766 Dielectric Mixing Models for Passive Microwave Soil Moisture Retrieval Using Data
767 From ComRAD Ground-Based SMAP Simulator. IEEE J. Sel. Top. Appl. Earth Obs.
768 Remote Sens. 8(9): 4345–4354. doi: 10.1109/JSTARS.2014.2372031.

769 Topp, G.C. 2003. State of the art of measuring soil water content. Hydrol. Process. 17(14):
770 2993–2996. doi: 10.1002/hyp.5148.

771 Topp, G.C., J.L. Davis, and A.P. Annan. 1980. Electromagnetic determination of soil water
772 content: Measurements in coaxial transmission lines. Water Resour. Res. 16(3): 574–
773 582. doi: 10.1029/WR016i003p00574.

774 Vaz, C.M.P., S. Jones, M. Meding, and M. Tuller. 2013. Evaluation of Standard Calibration
775 Functions for Eight Electromagnetic Soil Moisture Sensors. Vadose Zone J. 12(2): 0.
776 doi: 10.2136/vzj2012.0160.

777 Veeramanikandasamy, T., K. Sambath, K. Rajendran, and D. Sangeetha. 2014. Remote
778 monitoring and closed loop control system for social modernization in agricultural
779 system using GSM and Zigbee technology. 2014 International Conference on
780 Advances in Electrical Engineering (ICAEE). IEEE, Vellore, India. p. 1–4

781 Walker, J.P., G.R. Willgoose, and J.D. Kalma. 2004. In situ measurement of soil moisture: a
782 comparison of techniques. J. Hydrol. 293(1): 85–99. doi:
783 10.1016/j.jhydrol.2004.01.008.

784 Zhu, Y., S. Irmak, A.J. Jhala, M.C. Vuran, and A. Diotto. 2019. Time-domain and
785 Frequency-domain Reflectometry Type Soil Moisture Sensor Performance and Soil
786 Temperature Effects in Fine- and Coarse-textured Soils. Appl. Eng. Agric. 35(2):
787 117–134. doi: 10.13031/aea.12908.